Traffic 2010; **11:** 675–687

doi:10.1111/j.1600-0854.2010.01041.x

Cellular Internalization of Exosomes Occurs Through Phagocytosis

Du Feng†, Wen-Long Zhao†, Yun-Ying Ye, Xiao-Chen Bai, Rui-Qin Liu, Lei-Fu Chang, Qiang Zhou, Sen-Fang Sui*

School of Life Sciences, State Key Laboratory of Biomembrane and Membrane Biotechnology, Tsinghua University, Beijing 100084, PR China
**Corresponding author: Sen-Fang Sui, suisf@mail.tsinghua.edu.cn*
† *These authors contribute equally to this work.*

Exosomes play important roles in many physiological and pathological processes. However, the exosome–cell interaction mode and the intracellular trafficking pathway of exosomes in their recipient cells remain unclear. Here, we report that exosomes derived from K562 or MT4 cells are internalized more efficiently by phagocytes than by non-phagocytic cells. Most exosomes were observed attached to the plasma membrane of non-phagocytic cells, while in phagocytic cells these exosomes were found to enter via phagocytosis. Specifically, they moved to phagosomes together with phagocytic polystyrene carboxylate-modified latex beads (biospheres) and were further sorted into phagolysosomes. Moreover, exosome internalization was dependent on the actin cytoskeleton and phosphatidylinositol 3-kinase, and could be inhibited by the knockdown of dynamin2 or overexpression of a dominant-negative form of dynamin2. Further, antibody pretreatment assays demonstrated that tim4 but not tim1 was involved in exosomes uptake. We also found that exosomes did not enter the internalization pathway involving caveolae, macropinocytosis and clathrin-coated vesicles. Our observation that the cellular uptake of exosomes occurs through phagocytosis has important implications for exosome–cell interactions and the exosome intracellular trafficking pathway.

Key words: caveolin, clathrin, dynamin, early endosome, endocytosis, exosomes, late endosome, multivesicular body, phagosome

Received 27 July 2009, revised and accepted for publication 12 January 2010, published online 5 February 2010

Exosomes are membrane vesicles 30–100 nm in diameter that are released into the extracellular milieu upon the fusion of multivesicular bodies with the plasma membrane. These bioactive nanovesicles were originally described as part of the mechanism for the removal of transferrin receptor (TfR) during reticulocyte maturation (1). Following their discovery in reticulocytes by Johnstone et al., exosomes were also shown to be present in many cell types, including lymphocytes, epithelial cells, tumor cells, and neuronal cells (2–5). They are thought to play important roles in antigen presentation (6), cell transformation (7) and many other physiological and pathological processes (8,9). Exosomes bear a select subset of membrane proteins of endocytic origin, including many signaling ligands. The presence of exosomes in urine (10,11), circulating blood (12), ascites (13) and cerebrospinal fluid (14) *in vivo* suggests a role in intercellular communication (15,16). Indeed, Eaton et al. suggested that they may be a vehicle for the spread of morphogens through the epithelia (17). Several recent studies have indicated that exosomes can be utilized as shuttles by toxins (18,19), retroviruses (20,21) and prions (22,23); hijacked exosomes subsequently interact with recipient cells, which may arouse toxicity and infectivity or cause the spread of prions. Recent data indicate that exosomes enwrap messenger RNAs (mRNAs) and microRNAs, and that the mRNAs within exosomes are transferred to neighboring cells for translation (24). Surprisingly, exosomes from glioblastomal cells were found to transport RNA and proteins that promote tumor growth (25). The above functions are thought to rely mainly on the internalization and intracellular trafficking of exosomes followed by release of the message or the initiation of intracellular signaling. Although previous reports indicated that exosomes could be taken up by several cell types (26,27), how exosomes interact with recipient cells and how exosomes are sorted after entry into these cells remain unclear (28–30).

Here, we report that exosomes from untreated K562 (human erythroleukemia) or MT4 (HTLV-transformed T-cell leukemia) cells interact with different cells through two distinct modes. For phagocytic cells, they can be internalized efficiently via phagocytosis. For non-phagocytic cells, however, there are only a few intracellular exosomes and most exosomes attach to the cell membrane. We found that internalized exosomes are not only surrounded by cellular extensions and large phagosomes but are also internalized together with phagocytic tracers. The knockdown of dynamin2 (Dyn2), an important regulator of phagocytosis, almost completely inhibited exosome entry into the cell. Further, the colocalization of exosomes with phagolysosomal markers indicated that they are sorted into phagolysosomes. These findings shed new light on how exosomes interact with cells as well as the pathway leading to their internalization into cells.

Results

Exosomes from K562 or MT4 cells are internalized more efficiently by phagocytic cells than non-phagocytic cells

K562 cell- or MT4 cell-derived exosomes were purified for investigation. Their size, morphology and buoyant density were confirmed by electron microscopy and sucrose density gradient centrifugation as reported previously (Figure S1A,B) (31,32). K562 cell-derived exosomes were labeled with PKH26 as described (Figure S1C) (33,34) and further analyzed using immunogold-conjugated antibodies against tumor susceptibility gene 101 (*Tsg101*) and transferrin receptor (Figure S1D). MT4 cell-derived exosomes were purified according to the procedures of K562 cell-derived exosomes and labeled with PKH67 fluorescent dye (Figure S1E).

We first examined the interaction between exosomes and RAW 264.7 macrophages or mouse fibroblast NIH 3T3 cells. Our observations indicated that both kinds of exosomes were internalized efficiently by RAW 264.7 macrophages (Figure 1A,B, left panel). However, most of them tended to attach to the surface of the NIH 3T3 cells and could not be completely washed out with phosphate-buffered saline (PBS) alone (Figure 1A, right panel). Only a few intracellular exosomes were observed inside NIH 3T3 cells (Figure 1A,B). As a control, the internalization of transferrin was observed in both cell types, suggesting that the classic endocytic pathway was active (Figure 1B). In addition, we used polystyrene carboxylate-modified latex beads (biospheres) as phagocytic tracers to examine the phagocytic capability of the cells. As expected, RAW 264.7 macrophages, but not NIH 3T3 cells, showed effective internalization of beads (Figure 1B).

The observation that the exosomes interacted with the cells via two distinct modes prompted us to examine whether this is a common feature that can be applied to other cell types. Exosome internalization was examined in several cell types by trypsinization and acid washing. Surprisingly, in addition to RAW 264.7 macrophages, the exosomes also entered other phagocytic cells, including U937 monocyte-derived macrophages, THP-1 myelomonocytic cells and J774A.1 macrophages, as they could not be eliminated by trypsinization and treatment with citric acid buffer (Figure 1C). In contrast, only a few exosomes were internalized by non-phagocytic cells, such as Jurkat T cells, 293T cells, COS-7 kidney cells, HEL299 human lung fibroblasts, or mouse fibroblast NIH 3T3 cells (Figure 1C), as the surface-bound exosomes could be removed by trypsinization followed by several washes with citric acid buffer (Figure 1C).

Moreover, we studied the dynamics of exosome internalization. Exosome uptake was detected after 15 min and increased thereafter (Figure 1D). Consistent with the above observations, the dynamic curves of exosome internalization exhibited two distinct patterns corresponding to the two groups of cells. For the phagocytic cells, exosome uptake increased markedly with time, reaching a plateau after 12 h (Figure 1D,E). For the non-phagocytic cells, however, exosome uptake was almost not detected even after 24 h of incubation (Figure 1E). These observations exclude the possibility of delayed uptake in non-phagocytic cells.

Exosomes enter cells via an actin network- and PI3-kinase (PI3K)-dependent phagocytic pathway

To examine the exosome intracellular trafficking and sorting pathway, electron microscopy was used to trace the intracellular movement of internalized exosomes in phagocytic cells. Gold-labeled exosomes first attached to cellular extensions at the cell surface then were recruited to cup-like indentations and large cellular extensions that began to surround the exosomes (Figure 2A). However, in non-phagocytic NIH 3T3 cells, gold-labeled exosomes were bound only to the cell surface (Figure 2B); no intracellular exosomes could be detected (data not shown). After about 30 min of incubation, several gold-labeled exosomes were detected in phagosome-like compartments in macrophages with a diameter of 1 μm or greater (Figure 2C). Next, well-established phagocytic tracers (Biospheres, green) (35), together with PKH26-labeled exosomes (red) and transferrin (blue), were incubated with the macrophages. Almost all of the K562 cell- (Figure 2F,G) or MT4 cell- (Figure 3A) derived exosomes entered biospheres containing phagosomes; however, transferrin did not enter these structures. Further, live-cell imaging showed that PKH26-labeled exosomes (red spots) from K562 cells were seen to move along a cell synapse first, and then into the macrophage (green) (Movie S1). Ultrastructural analysis showed that the gold-labeled exosomes and phagocytic tracers began to be cointernalized after about 10 min of incubation (Figure 2D), after which they moved deeper inside the cell and were surrounded by large smooth-surfaced phagosomes within 30 min (Figures 2E and 3B).

As actin polymerization is required for phagosome formation (36), we next examined the role of the actin cytoskeleton in exosome uptake by RAW 264.7 macrophages. Cells were pretreated with cytochalasin D (Cyto D) or latrunculin B (Lat B), both of which are inhibitors of actin polymerization (37,38). Exosome internalization was significantly restricted in a dose-dependent manner following treatment with Cyto D or Lat B; in the presence of 0.5 and 1 μM Cyto D or Lat B, internalization was decreased by 38 ± 10% and 75 ± 5% or 45 ± 9% and 72 ± 7%, respectively; both drugs inhibited exosome uptake almost completely at 5 μM (Figure 2H). The inhibition of exosome entry was not because of toxic effects on the macrophages, as neither drug affected macrophage viability (data not shown).

PI3-kinases (PI3Ks) are essential for phagocytic processes (39), and their primary role in phagocytosis appears to be in facilitating membrane insertion into forming

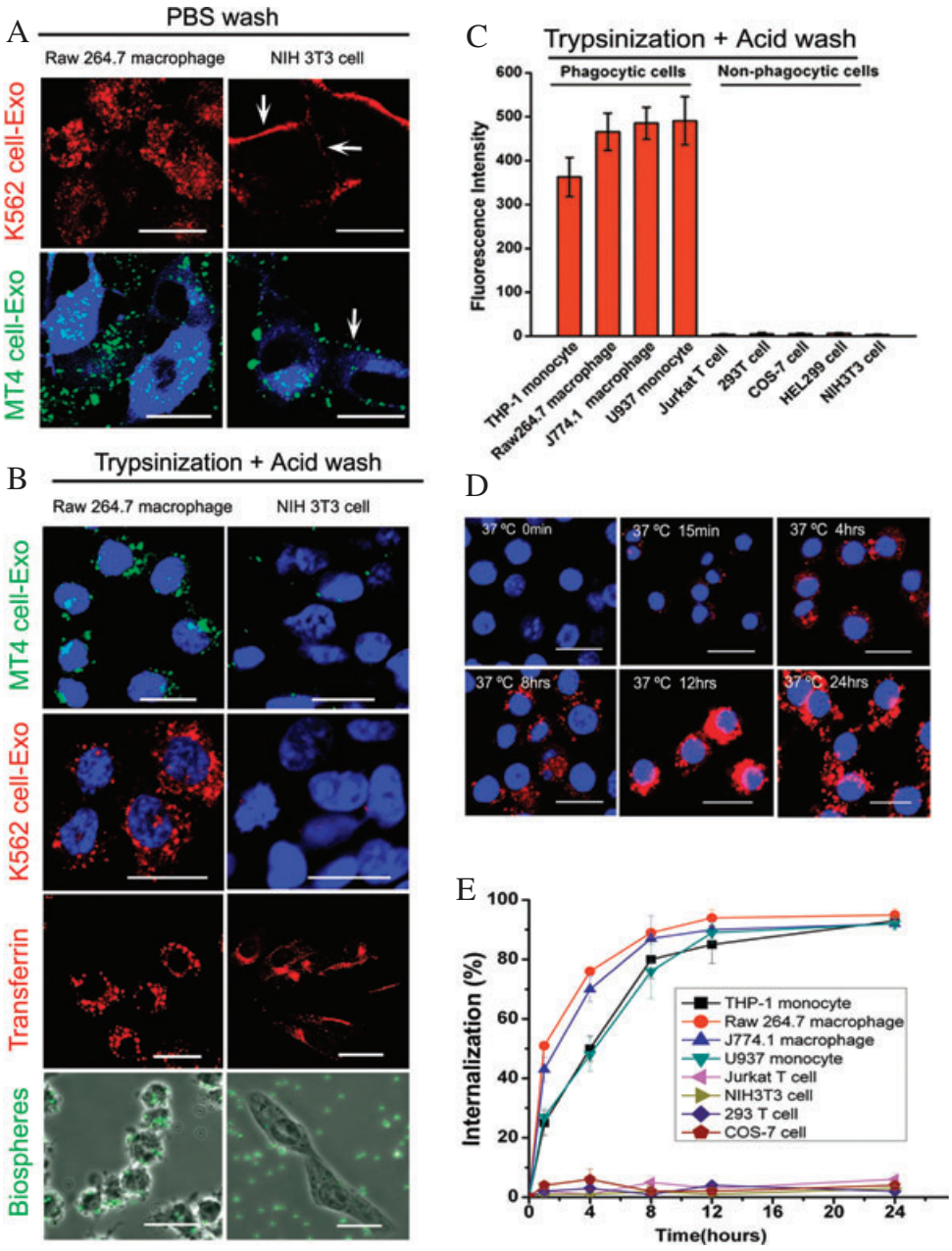

Figure 1: Exosomes from K562 or MT4 cells are internalized more efficiently by phagocytic cells than non-phagocytic cells. A) RAW 264.7 macrophages or NIH 3T3 cells were incubated with PKH26-labeled exosomes (red, upper panel) from K562 cells or PKH67-labeled exosomes (green, lower panel) from MT4 cells at 37°C for 60 min, washed three times with PBS and analyzed by confocal microscopy. Arrows indicate exosomes bound to the surface of NIH 3T3 cells. NIH 3T3 cells (lower panel) were stained by CellTracker (sigma) and designated as blue. Scale bar, 20 μm. B) RAW 264.7 macrophages or NIH 3T3 cells were incubated with PKH26-labeled exosomes from K562 cells or PKH67-labeled exosomes from MT4 cells for 3 h, transferrin for 15 min or biospheres (phagocytic tracers) for 30 min. After incubation, cells were treated with 0.2× tripsin/EDTA buffer for 1 min and then washed extensively with citric acid buffer to remove all non-endocytosed transferrin, biospheres, or exosomes bound to the cell surface. Nuclei (blue) were stained with DAPI. Scale bar, 20 μm. C) Cells were incubated with PKH26-labeled exosomes which were derived from K562 cells for 4 h, and then tripsinized and washed extensively with citric acid buffer to remove surface-bound exosomes. Exosome uptake was measured by determining the fluorescence intensity. The data represent the mean ± SD of three independent experiments. D,E) Phagocytic and non-phagocytic cells were incubated with PKH26-labeled exosomes for various time periods. After washing, the samples were either subjected to confocal laser scanning microscopy or analyzed using a luminometer. Nuclei (blue) in (D) were stained with DAPI. The data are expressed as the mean ± SD of three independent experiments. Scale bar in (D), 20 μm.

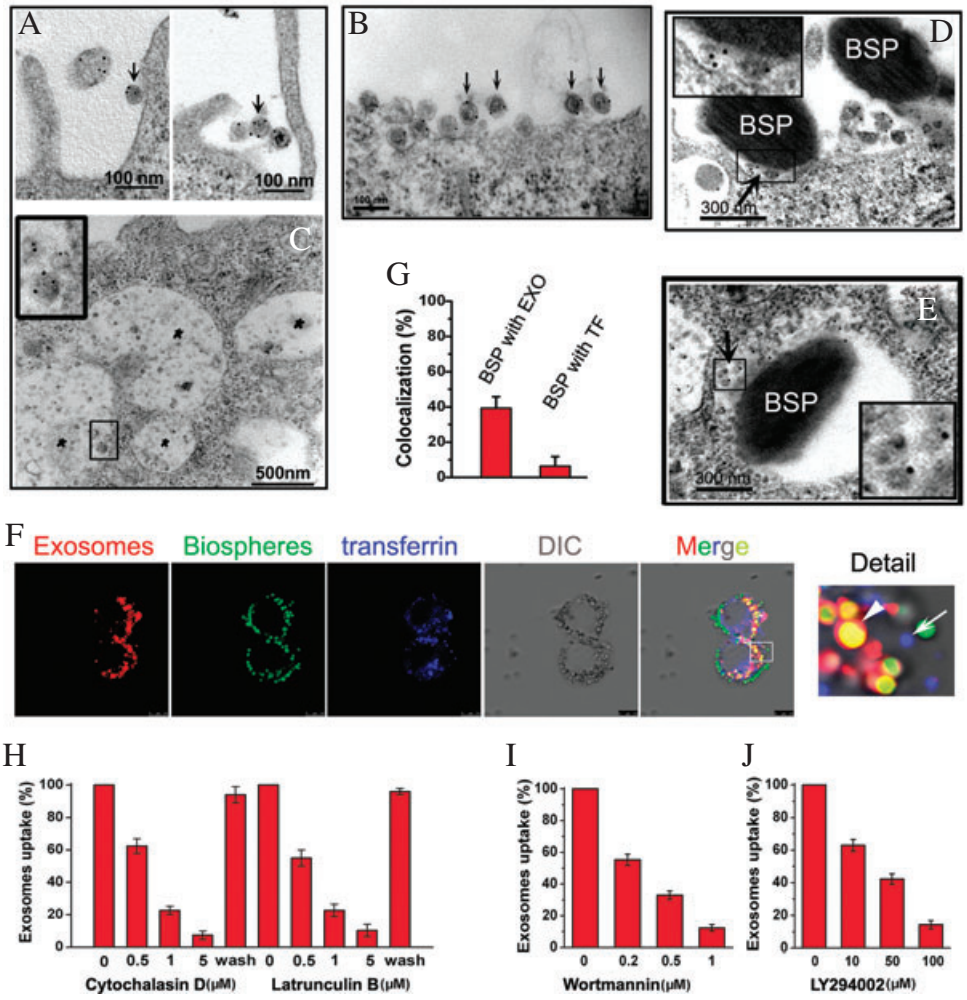

Figure 2: Exosomes enter cells through an actin network- and PI3K-dependent phagocytic pathway. Exosomes from K562 cells were prelabeled by anti-TfR antibody, then by second antibody conjugated to 12-nm protein A-gold. (A) Exosomes attached to cellular extensions of RAW 264.7 macrophage (left panel). Cup-like indentations formed at the RAW 264.7 macrophage cell surface and large cellular extensions began to surround the exosomes (right panel). The arrows in (A) indicate 12-nm gold-labeled exosomes. (B) Exosomes were present on the surface of non-phagocytic NIH 3T3 cells. Twelve-nanometer gold-labeled exosomes were incubated with the cells for 2 h at 37°C, after which the samples were washed and processed for electron microscopy. Arrows indicate exosomes bound to the plasma membrane. (C) Large smooth-surfaced phagosomes containing exosomes were seen in RAW 264.7 macrophage. Asterisks indicate giant phagosomes containing exosomes. (D, E) Exosomes were incubated with phagocytic tracers (biospheres) for 10 min (D) or 30 min (E), and colocalization of phagocytic tracers (biospheres) with internalized 12-nm gold-labeled exosomes were shown. The insets show internalized 12-nm gold-labeled exosomes (arrows). BSP, biosphere. (F) PKH26-exosomes (red), phagocytic tracers (green) and Alexa Fluor-transferrin (blue) were coincubated with macrophages at 37°C for 45 min, washed, fixed and subjected to confocal laser scanning microscopy. White arrowhead indicates exosomes colocalized with biospheres; white arrow is transferrin. Bar, 7.5 μm. (G) The colocalization of biospheres with exosomes and transferrin was quantified in 30 cells. (H) Macrophages were treated with various concentrations of Cyto D or Lat B for 30 min, then incubated with exosomes for 2 h or washed out after 2 h. The exosomes were visualized and quantified based on their fluorescence intensity. The results, expressed as the percentage of exosome uptake relative to the control, are the means ± SD of three experiments. (I) and (J) RAW 264.7 macrophages were pretreated with various concentrations of wortmannin or LY294002 for 30 min and then incubated with exosomes for 2 h in the presence of either drug. Internalization of the exosomes was quantified based on the fluorescence intensity. The results, expressed as the percentage of exosomes relative to the control, are the means ± SD of three independent experiments.

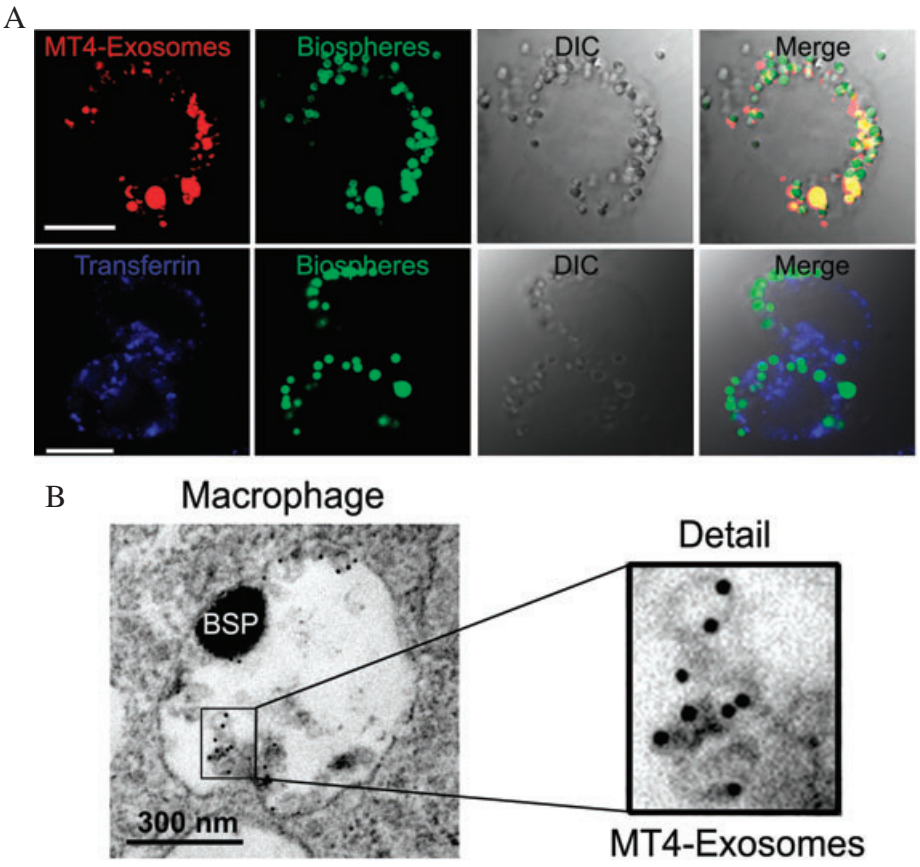

Figure 3: MT4 cell-derived exosomes co-internalize with phagocytic tracers. A) In macrophages, fluorescent phagocytic tracers (green) were incubated with PKH26-exosomes (red) derived from MT4 cell (upper panel) or Alexa Fluo-633-transferrin (blue) at 37°C for 30 min, washed, fixed and subjected to confocal laser scanning microscopy. Bars, 15 μm. B) Colocalization of phagocytic tracers (biospheres) with internalized 12-nm gold-labeled exosomes. The insets (left) and detail (right) show internalized 12-nm gold-labeled exosomes. BSP, biosphere.

phagosomes (40). Therefore, we examined the potential role of PI3Ks in exosome entry using two potent PI3K inhibitors, wortmannin and LY294002. As expected, both drugs inhibited the internalization of exosomes in a dose-dependent manner (Figure 2I,J).

Taken together, these results clearly indicate that the entry of exosomes into macrophages occurs through phagocytosis.

Phagocytosis of exosomes by mouse macrophages is partially reduced by TIM-4 but not TIM-1 antibody

Recently, Miyanishi et al. identified TIM-4 and TIM-1 as endogenous phagocytic receptors for apoptotic cells (41). The authors also indicated the role of TIM-4 in cellular phagocytosis of exosomes because previous reports demonstrated that phosphatidylserine could be found on microvesicles (including exosomes) (27,42,43). To assess the involvement of TIM-4 and TIM-1 in phagocytosis of exosomes, we preincubated RAW264.7 cells with either TIM-4 or TIM-1 antibody alone, or both of them, or isotype control. Macrophages were then co-cultured with PKH67-labeled exosomes for 60 min. For confocal observation, cells were further labeled by dylight-633 conjugated second antibodies (Figure 4A). Phagocytosis was measured by flow cytometry (Figure 4B). Compared to isotype control antibody, the percentage of phagocytosed exosomes was reduced by 30 ± 10% by 5 mg/mL of TIM-4 antibody. In contrast, TIM-1-antibody-mediated reduction was only 5 ± 4%; a combined use of the antibodies inhibited exosomes entry by 37 ± 8% (Figure 4B). These results suggested that TIM-4 but not TIM-1 might be one of the receptors used by mouse macrophages to recognize and phagocytose exosomes.

Exosomes are sorted to phagolysosomes

Phagosomes tend to fuse with lysosomes to form phagolysosomes, whose maturation is signaled by the acquisition of lyso-bis-phosphatidic acid (LBPA), Rab7 and lysosomal-associated membrane proteins (LAMPs) (44,45). Therefore, we examined whether phagocytosed exosomes can be sorted into phagolysosomal compartments. RAW 264.7 macrophages were incubated with exosomes for various time periods, and colocalization of the exosomes with phagolysosomal markers was assessed by immunofluorescence and confocal microscopy. As shown in Figure 5, most exosomes entered the compartments where they clearly colocalized with Lamp-1, LBPA and Rab7 (Figure 5A). Quantitative analysis indicated the overlap to be 65 ± 9% with Lamp-1, 48 ± 5% with LBPA and 37 ± 7% with Rab7 (Figure 5C). In addition, spinning disc confocal live-cell microscopy confirmed that Rab7-positive vesicles could fuse with exosome-containing phagosomes (Figure 5B, Movie S2).

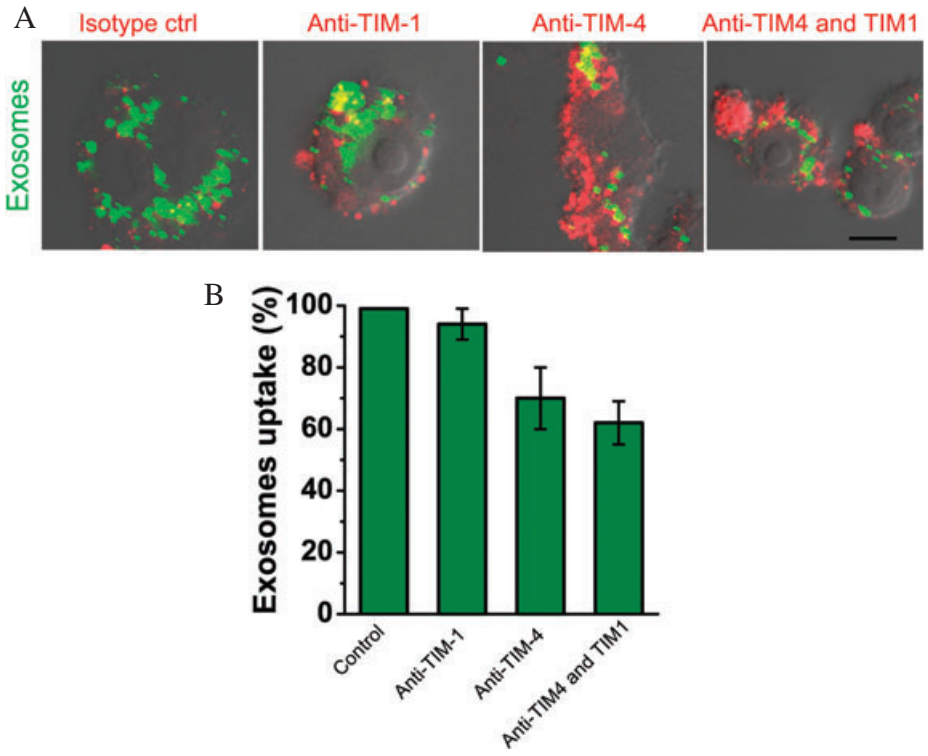

Figure 4: TIM-4 but not TIM-1 antibody partially inhibited phagocytosis of exosomes by mouse macrophages. A) Mouse RAW264.7 cells were preincubated with 5 mg/mL isotype control, TIM-1 antibody, TIM-4 antibody or both TIM-1 and TIM-4 antibodies for 10 min followed by PKH67-labeled exosomes for 30 min. Non-internalized exosomes were removed by acid washing. Cells were further labeled by Dylight-633 conjugated second antibodies and examined by confocal microscopy. Images are representative of three experiments. Bar, 20 μm. B) Quantification of phagocytosis of exosomes by flow cytomerty. Data are shown as mean ± SD of duplicate wells and are representative of three independent experiments.

No colocalization was observed between the exosomes and the endoplasmic reticulum (ER) marker calnexin or the Golgi marker Rab6, suggesting that phagocytosed exosomes did not enter the retrograde transport pathway (Figure S2). Taken together, our results indicate that exosomes are targeted to phagolysosomes.

Dyn2 is required for exosome internalization

As Dyn2 is a key player necessary for clathrin-, caveolin-dependent endocytosis and phagocytosis but not involved in macropinocytosis (46,47), its role in exosome internalization was examined in RAW 264.7 macrophages transfected with wild-type dynamin2 (Dyn2WT) or a dominant-negative version of (Dyn2K44A). Phagocytic tracers (biospheres) were used as a positive control. Dyn2K44A expression inhibited biospheres internalization by 65% and exosome internalization by 81% compared with the Dyn2WT transfectants. As a negative control, exosomes were not internalized by macrophages on ice, irrespective of Dyn2WT and Dyn2K44A transfectants (Figure 6A). The same effects of Dyn2WT and Dyn2K44A on exosome internalization were observed by confocal microscopy (Figure 6B). Next, Dyn2 was successfully knocked down by short interfering RNA (siRNA) (Figure 6C, upper panel). In the dynamin-negative cells, exosome internalization was almost completely blocked, while normal exosome uptake was observed in the dynamin-positive cells (Figure 6C, lower panel).

Taken together, the above results indicate that Dyn2 is essential for the cellular internalization of exosomes.

Role of Clathrin and Caveolin-1 in exosomes uptake

Caveolin1 and clathrin, which are involved in the early steps of cellular internalization (48,49), were also examined. Macrophages were incubated with exosomes for 10 min. Then clathrin-coated vesicles were labeled by anti-clathrin antibody. About 8 ± 5% of exosomes containing vesicles colocalized with clathrin at 10 min (Figure S3A,C). The percentage of colocalization then decreased to 5 ± 1% at 30 min, and finally to 3 ± 2% at 60 min (Figure S3A,C). Overall, only a small fraction of internalized exosomes associated with clathrin; likewise, the exosomes did not enter the caveolae during the early stages of internalization (Figure S3B,C)

To further assess the role of clathrin in exosomes internalization by macrophages, we expressed dominant-negative mutant GFP-Eps15 E Δ 95/295 (Eps15 mt), which interferes with clathrin-coated pit assembly (50), Eps15 control or green fluorescent protein (GFP). We found that Eps15 mutant transfectants still internalize exosomes: 75 ± 6% of exosomes were internalized by macrophages compared to 95 ± 5% of Eps15 control and 100% of GFP-expressing macrophages, although, the internalization of transferrin was dramatically impaired (Figure 7A,B). As an alternative approach, we used chlorpromazine to inhibit clathrin-mediated endocytosis (51). The activity of chlorpromazine was tested through the inhibition of transferrin uptake. Chlorpromazine inhibited transferrin uptake in a dose-dependent manner with 50 μM chlorpromazine mediating 82 ± 5% inhibition (Figure 7C,D), while exosomes uptake in RAW 264.7 macrophages was only inhibited by 24 ± 7% at 50 μM (Figure 7C,D).

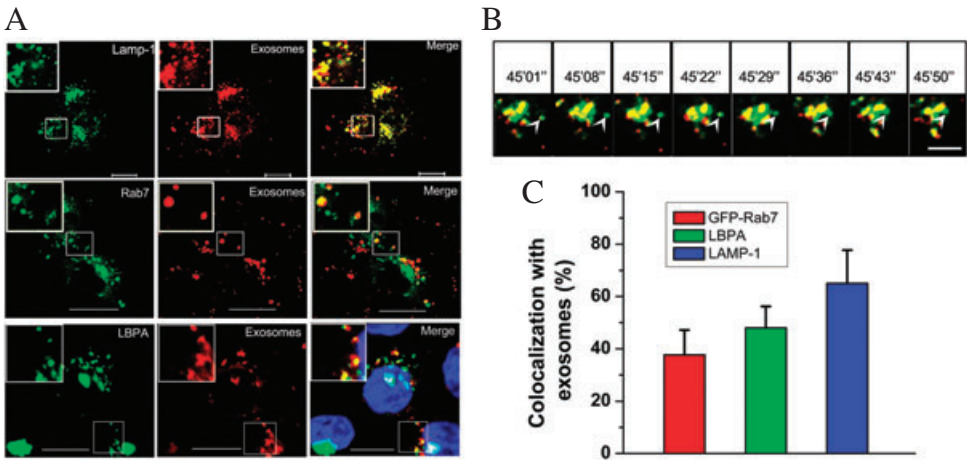

Figure 5: Exosomes traffic to phagolysosomes. A) Macrophages were incubated with exosomes at 37°C for 2 h, washed and then immunolabeled for LBPA, Lamp1 or Rab7. Laser scanning confocal images are shown (yellow indicates colocalization of the green and red signals); the nuclei were stained with DAPI (blue). Scale bar, 10 μm. B) To observe the process that exosomes containing compartment fuse with Rab7-EGFP-positive vesicles directly, we first let Rab7-EGFP-transfected RAW264.7 macrophages actively internalize exosomes at 37°C and then non-internalized exosomes were washed out by complete medium. A series of frames were taken with a live-cell imaging CCD camera. Arrowheads indicate a moving Rab7-positive vesicle (green) that subsequently fused with an organelle (yellow–green) already enwrapping exosomes. Scale bar, 2 μm. C) Quantification of the colocalization with each phagolysosomal marker in 20 cells. The values given are the means ± SD of three independent experiments.

Taken together, these data suggest clathrin-mediated endocytosis plays a minor role in exosomes uptake and caveolin-1 is not involved in exosomes uptake.

Role of macropinocytosis in exosomes uptake

To investigate the role of macropinocytosis in the entry of exosomes into macrophages, we first studied the colocalization of exosomes with fluorescein isothiocyanate (FITC)-dextran, a marker of macropinocytosis. As shown in Figure 8A,C, the percentage of colocalization of exosomes with FITC-dextran is only 16 ± 5%. Second, we studied the effect of an inhibitor of macropinocytosis on exosomes uptake. 5-ethyl-N-isopropyl amiloride (EIPA) is a specific inhibitor of macropinocytosis that blocks Na+/H+ exchange (52,53). EIPA activity was tested through the inhibition of FITC-dextran uptake. RAW 264.7 macrophages were first pretreated with different doses of EIPA for 30 min, and then incubated with exosomes or FITC-dextran in the presence of EIPA. Their uptake was determined by fluorescence intensity. Exosomes uptake was not affected by EIPA, regardless of its concentration (Figure 8B,D). As a positive control, EIPA at 200 μM successfully inhibited FITC-dextran uptake (Figure 8B,D).

Taken together, these results showed that exosomes enter macrophages not through macropinocytosis.

Discussion

In this study, exosome internalization, intracellular sorting and trafficking were examined in detail. First, we found that exosomes are taken up more efficiently by phagocytic cells than non-phagocytic cells, which suggests that phagocytic capability is essential for exosome uptake, and thus accounts for the different exosome–cell interaction modes. Indeed, after phagocytosis, exosomes are targeted to large phagolysosomes. Second, the roles of dynamin, clathrin and caveolin were investigated. The exosomes required dynamin in the initial stage of phagocytosis, during which a minimal fraction of exosomes associated with clathrin but were not sorted to the caveolae, macropinosome, ER or Golgi during uptake.

Exosomes have been the subject of a number of studies, including their biogenesis and function, but their fate after release into the extracellular milieu remains unclear (29). The abundant information they carry and their complicated functions may have a marked impact on cells in three ways: binding to the cell surface, direct fusion with the plasma membrane, and/or internalization by recipient cells (54).

With regard to the proposed binding and internalization modes, it was reported that exosomes can be internalized and processed by immature dendritic cells (27). On the other hand, human tumor nanoparticles can induce apoptosis in cancer cells mainly through direct binding to the lipid rafts of the plasma membrane, which may trigger an apoptotic signaling cascade (55). The reason why some cells can take up these nanovesicles while others cannot has not been elucidated. Recently, Tumne et al. demonstrated that exosomes secreted from CD8+ T cells suppressed HIV-1 transcription in HeLa cells through direct binding but not internalization (56), while

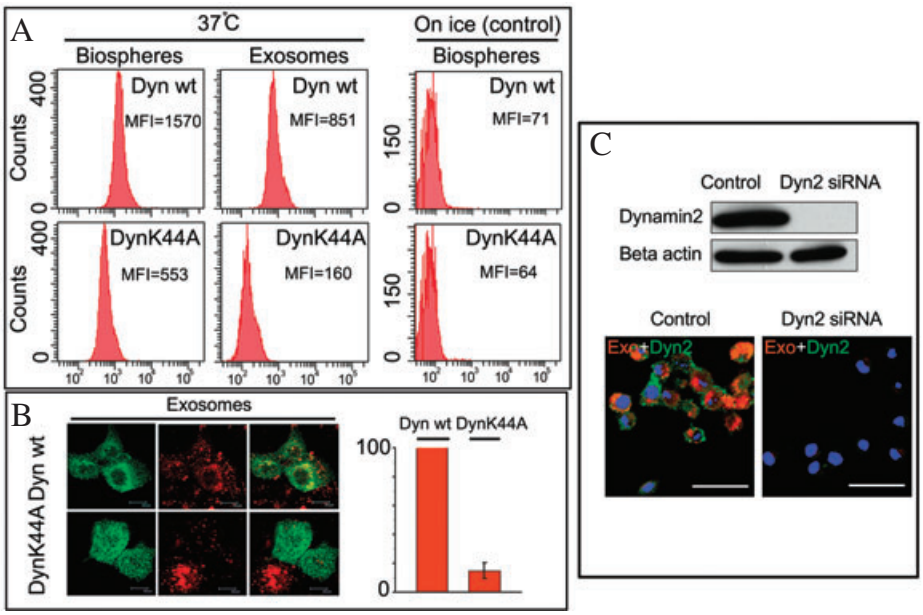

Figure 6: Exosome internalization is dynamin-dependent. A) Cells transfected with GFP-tagged Dyn2WT or GFP-tagged Dyn2K44A were incubated at 37°C with phagocytic biospheres for 30 min or with PKH26-labeled exosomes for 60 min to allow for endocytosis, trypsinized and subjected to acid washing. Next, aliquots of 5×10^6 cells internalizing phagocytic biospheres or PKH26-labeled exosomes were examined by FACS. The cells that were analyzed were gated on GFP+ cells that expressed the dynamin transgenes. Vertically, both the left two and the right two panels, the signal was derived from the red fluorescent biospheres (the same channel as PKH26 dye); vertically, two panels in the middle, the signal was derived from red fluorescent PKH26-labeled exosomes. Mean fluorescence intensity (MFI) values for each sample is provided in each of the panels. The data were obtained from three independent experiments; representative FACS images are shown. B) Both the Dyn2WT- and Dyn2K44A-transfected cells were incubated with PKH26-labeled exosomes for 120 min, acid washed and subjected to confocal laser scanning microscopy on coverslips. Five images were scanned from the top to the bottom of a cell and combined as a whole image which may represent the total exosomes uptake efficiency in both dynamin wild type and mutant cells. Scale bar, 20 μm. The histogram shows the effects of two different constructs on exosome uptake. The number of internalized exosomes was determined based on the integrated fluorescence inside 80–100 cells. The results are expressed as the mean ± SEM of three independent experiments. C) Cells were transfected with siRNA against Dyn2 or with scrambled siRNA (Control). Western blotting was performed on protein extracts from aliquots of 10^6 cells with antibodies against Dyn2 or against β-actin as a loading control. The transfected cells were incubated with exosomes (red) for 2 h, subjected to acid washing, and probed with an antibody against Dyn2 (green). Scale bar, 40 μm.

Khatua et al. reported that internalization was essential for the exosomal packaging of APOBEC3G, which confers HIV-1 resistance on HeLa cells (57). In our experiments, exosomes adhered easily to the cell surface of non-phagocytic cells during incubation and could not be washed off with PBS. Under microscopy this would cause an artifact observation; they actually remained on the plasma membrane. Using live-cell imaging combined with biochemical and ultrastructural analyses, we produced direct evidence that exosomes cannot be internalized efficiently by a broad array of non-phagocytic cells but only associate with their plasma membranes, as they could be removed by trypsinization or with extensive acid washing. In contrast, the same treatment did not remove exosomes from phagocytes as they were already inside the cell. Hence, our observations account for the different mechanisms by which exosomes interact with cells. We conclude that phagocytic capability is essential for these classes of exosome internalization. Of course, there is a possibility that exosomes from other sources might have cargoes that facilitate internalization by other uptake mechanisms. Indeed, several different receptors mediating exosome internalization have been reported recently (41,58,59). Likewise, cells which are specialized for macropinocytosis (e.g. DC) might use macropinocytosis or other mechanisms for exosome uptake, even for these same classes of exosomes. In non-phagocytic cells, binding may be sufficient for the signaling triggered by exosomes (55,60). For example, the recruitment of exosomes from mature dendritic cells by activated T cells via LFA-1 (58) and ICAM-1 is critical for efficient naïve T-cell priming (59), while for professional phagocytes, exosomes can be internalized for the ultimate signaling transport. T84-intestinal epithelial exosomes bear major histocompatibility complex (MHC) Class II/peptide complexes that serve in antigen presentation by dendritic cells (61). Hence, alternative exosome–cell interaction modes may be directly related to either their sources or their functions (27,58).

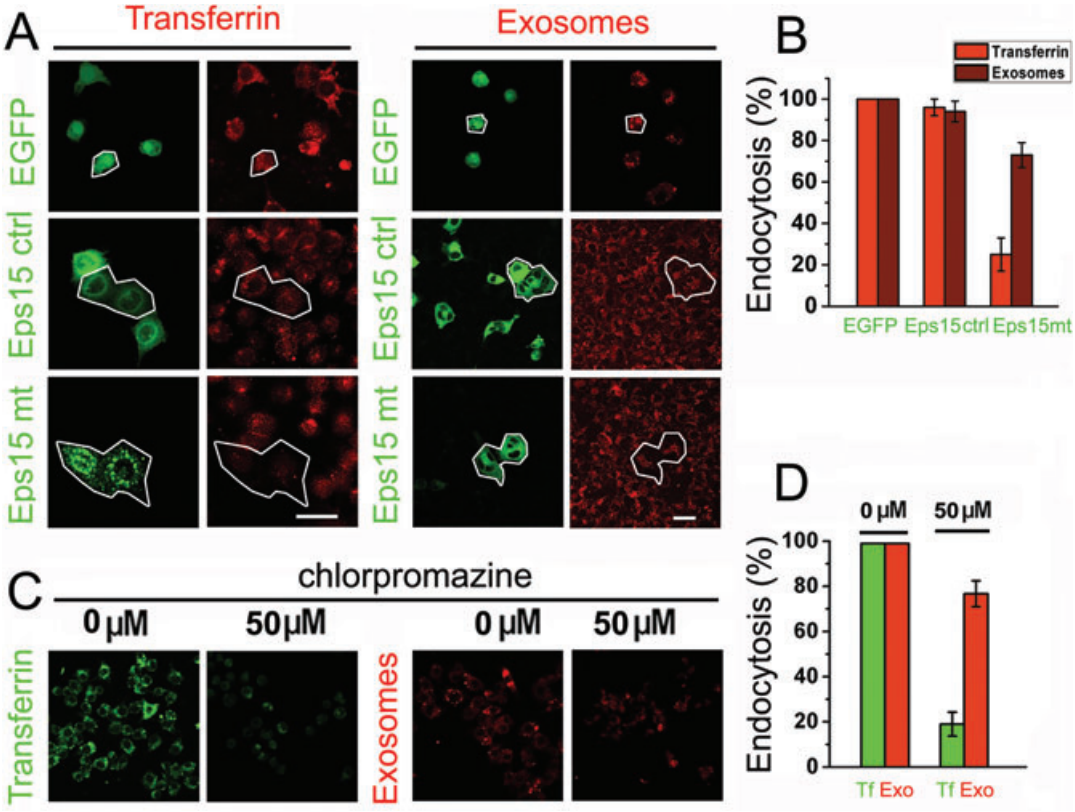

Figure 7: Role of clathrin in exosomes uptake. A) Macrophages were transfected with GFP, GFP-Eps15 DIII Δ 2 (Eps15 ctrl), GFP-Eps15 E Δ 95/295 (Eps15 mt). After transfection, cells were either incubated with AF594-Transferrin for 20 min or PKH26-exosomes for 2 h, fixed, and examined by confocal microscopy. AF594-Transferrin served as a positive control. Representative images are shown. Bars, 40 µm. B) Internalization of transferrin or exosomes was quantified. The results, expressed as the percentage of transferrin or exosomes relative to the control, are the means ± SD of three independent experiments. C) RAW 264.7 macrophages were pretreated with 50 µM chlorpromazine for 30 min and incubated with 50 µg/mL Alexa 488-conjugated transferrin for 15 min or PKH26-exosomes for 2 h. The intracellular distribution of fluorescent transferrin or exosomes was studied in control macrophages (left panels) and in 50 µM chlorpromazine-pretreated macrophages (right panels). Scale bars represent 50 µm. D) Internalization of transferrin or exosomes was quantified by FACS. The results, expressed as the percentage of transferrin or exosomes relative to the control, are the means ± SD of four independent experiments.

Although a recent study described that direct fusion may take place between exosomes and the plasma membrane (62), direct evidence using live-cell imaging or other related fluorescence techniques for this are still lacking (29,31).

During erythropoiesis, reticulocytes release small membrane vesicles termed exosomes (63). Erythrocytes are known to be phagocytosed after about four months in the circulation; however, the erythrocyte responsible for this release does not itself degrade the released vesicles, and the question arises as to how these exosomes are removed once they are released into the circulation *in vivo*. The observations presented here indicate that exosomes derived from K562 cells are only phagocytosed by professional phagocytes. This finding provides new insight into how these nanovesicles are eliminated from the bloodstream.

Materials and Methods

Cell culture, antibodies and reagents

Media and reagents for cell culture were purchased from GIBCO BRL. All cells were purchased from the American Type Tissue Collection unless otherwise stated. Mouse RAW 264.7 macrophages, J774A.1 macrophages, 293T cells, NIH3T3 cells, HEL299 cells and COS-7 cells were grown in Dulbecco's Modified Eagle Medium (DMEM) high glucose containing 10% fetal calf serum (FCS). K562 cells, MT4 cells, U937 cells and Jurkat T cells were grown in RPMI 1640 containing 10% FCS. MT4 is a HTLV-1 transformed T-lymphoblastoid cell line which was bought from NIH. Antibodies were obtained from the following sources: antibody against Clathrin heavy chain (CHC) and Dyn2are purchased from Cell Signaling Technologies. Antiserum against LBPA was provided by Jean Gruenberg (University of Geneva, Switzerland); antibodies against Calnexin, LAMP1, Rab7, Tansferrin receptor, Beta actin and Rab6 are all from Santa Cruz Biotechnology; antibodies against mouse TIM-1, TIM-4 and isotype control are bought from Biolegend. All fluorescently labeled ligands were obtained from Molecular Probes. Protein A-gold with dimensions 6 and 12 nm were purchased from Jackson ImmunoResearch. Polystyrene carboxylate-modified latex beads (biospheres) were bought from Sigma-Aldrich.

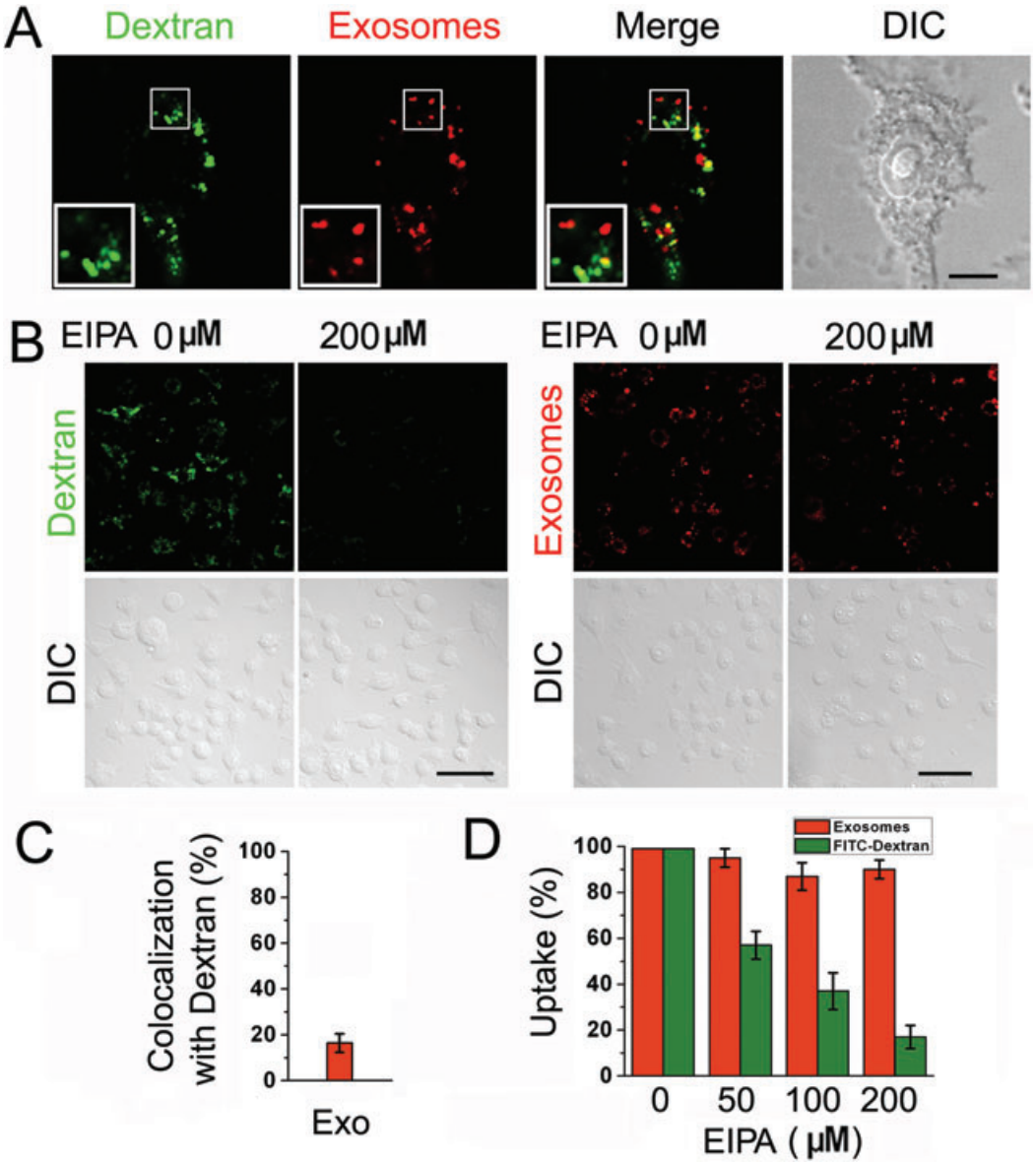

Figure 8: Role of macropinocytosis in exosomes internalization. A) Macropinocytosis marker (FITC-dextran) does not colocalize with exosome. RAW 264.7 macrophages were incubated with both 3 mg/mL FITC-dextran and 30 μg/mL exosomes for 30 min. The colocalization of FITC-dextran and exosome was demonstrated by merging fluorescent images. Scale bars, 25 μm. B) RAW 264.7 macrophages were mock treated or pretreated with 100 μM EIPA for 30 min and incubated with 3 mg/mL FITC-dextran for 30 min or 30 μg/mL PKH26-exosomes for 2 h. The intracellular distribution of fluorescent dextran or exosomes was studied in mock-treated control macrophages (left panels) and in 200 μM EIPA-pretreated macrophages (right panels). Scale bars, 60 μm. C) Colocalization of the exosome with FITC-dextran was quantified inside 30 cells. The values given are the means ± SD of three independent experiments. D) Macrophages were pretreated with different concentrations of EIPA and incubated with FITC-dextran or PKH26-exosomes. The mean fluorescence intensity was measured by FACS. The results, expressed as the percentage of dextran or exosomes uptake relative to the control, are the mean ± SD of three independent experiments.

Exosomes purification and labeling

K562 and MT4 cells were maitained in RPMI 1640 medium with exosome-free FCS. Exosomes were isolated from 2×10^8 cell culture medium collected after 24 h by differential centrifugations as described by Raposo and colleagues with a brief modification (2). Briefly, the collected culture mixture was centrifuged at 300 × ***g*** for 10 min, 800 × ***g*** twice for 15 min and 10 000 × ***g*** for 30 min to remove cells and debris. The supernatant was further filtered by a 0.22-μM filter, ultrafiltrated and condensed through Amicon Ultra-15 (Millipore). The condensed medium was centrifugated at 100 000 × ***g*** for 60 min on top of 1.6 mL of 30% sucrose density cushion to pellet exosomes. The phase containing the exosomes was collected, washed with large volume of PBS, ultracentrifugated, and the pellet was resuspended in PBS. Purified exosomes were labeled with PKH26 or PKH67 red fluorescent labeling kit (Sigma-Aldrich) as described

previously (33,34). The amount of exosome protein was assessed by Bradford assay (Bio-Rad).

Constructs and transfections

Dynamin2 wild type and Dyn2K44A plasmid constructs, both GFP-tagged, were kindly provided by Dr. M. McNiven (46) (Mayo Clinic and Foundation, Rochester, USA) and Lucas Pelkmans (64) (ETH Zurich, Switzerland). The EGFP-Clathrin-light-chain construct (Clathrin-EGFP) was a gift from Dr. James Keen (Thomas Jefferson University, Philadelphia, USA) (65). Caveolin-1-GFP (Cav-1-GFP) constructs were prepared as previously described (66). Eps15 plasmids were kindly provided by Dr. A. Benmerah (INSERM, Paris, France). Rab7-EGFP was cloned according to Vitelli and colleagues (67). RAW 264.7 macrophages were transfected with Dyn2WT, Dyn2K44A, Cav-1-GFP and Clathrin-EGFP plasmid constructs using Nucleofactor (Amaxa Biosystems), according to the manufacturer's recommendations.

Short interfering RNA

Dynamin2 siRNA sequences were directed against Dyn2 at coding regions 1732–1753 as oligo 1, 318–338 as oligo 2 and 173–193 as oligo 3. The oligos which exibited the best inhibition effect and the scrambled siRNA (control) were transfected by using oligofectamine (Invitrogen) as described by the manufacturer. Cells were transfected with 120 pmol of siRNA duplex per well in 6-well plates. SiRNA efficiency was tested by western blot using enhanced chemoluminescence (Pierce).

Endocytosis, immunofluorescence, confocal microscopy, and live-cell imaging

For internalization assay, cells were grown to subconfluency on coverslips and incubated with PKH26 labeled exosomes (5 μg per 60 000 cells), transferrin (5 μg/mL), or biospheres (1×10^8/mL) diluted in medium for the indicated times at 37°C, washed by either PBS or acid citrate buffer. For cells grown in suspension (K562, U937, MT4 and Jurkat T), washes were done in 5-mL tube; for adherent cells (RAW 264.7 macrophages, J774A.1 macrophages, 293T cells, NIH3T3 cells, HEL299 cells and COS-7 cells), washes were carried out either in 5-mL tubes after detaching the cells from monolayer (for fluorescence quantification) or directly in 6-hole culture dishes with 0.2× tripsin/EDTA for 1 min and citric acid (for confocal microscopy). Each of the samples was analyzed for internalization by confocal microscopy or luminometer. PKH26-labeled exosomes, or biospheres were incubated at 37°C for indicated times with cells which transfected with dynamin constructs or siRNAs targeting Dyn2, washed by acid citrate buffer, and fixed with 2.5% formaldehyde for 15 min. For colocalization experiments, samples were permeabilized with 0.05% (w/v) saponin/PBS and stained with the respective antibodies followed by FITC-labeled secondary antibodies. After mounting in anti-fade solution (Roche), coverslips were examined using an LSM510 ZEISS laser scanning confocal microscopy. For a given experiment, all the settings on the microscope were kept constant for all the samples, including exposures, pinhole size and photomultiplier tube (PMT) gain. Each experiment was repeated three times and for each individual experiment, all the samples were scanned at six different locations. Digital images were produced using the MetaMorph Offline software 6.1 (Universal Imaging Corp), Adobe Photoshop 8 (Adobe Systems Inc.). Colocalization events were calculated using the MetaMorph 6.0 software as described in the manufacturer's recommendations.

To observe the process that exosomes containing compartment fuse with Rab7-EGFP-positive vesicles directly, we let Rab7-EGFP-transfected RAW264.7 macrophages actively internalize exosomes at first at 37°C, then live-cell confocal time-lapse sequences were taken on a spinning disk confocal microscope system equipped with a 50-mW Krypton-Argon ion laser that delivered its radiation by a single fiber optic to a Yokogawa spinning disk confocal scan-head (Andor Revolution). The system used a IX81 inverted microscope (Olympus) with a 63× oil, numerical aperture (NA) = 1.4 Plan Apochromat differential interference objective lens and an Andor iXon+ 897 eletron multiplying charge-coupled device (EMCCD). ANDOR IQ software controlled the microscope functions and was used for image processing.

Flow cytometry

The FACS assay was carried out on BD FACSAria II (BD Biosciences) according to the manufacturer's recommendations. The dynamin and clathrin inhibition assay was performed as described previously. Briefly, RAW 264.7 macrophages were pretreated with 50 μM chlorpromazine for 30 min and incubated with 50 μg/mL Alexa 488-conjugated transferrin for 15 min or PKH26-exosomes for 2 h. Then, aliquots of 1×10^6drug–treated- or untreated cells internalizing Alexa 488-conjugated transferrin or PKH26-labeled exosomes were examined by FACS.

Drug treatments

Cells were preincubated for 30 min at 37°C in DMEM complete medium containing 0–5 μM Lat B or Cytochanasin D (Sigma-Aldrich), 0–1 μM Wortmannin or 0–100 μM LY294002 (Sigma-Aldrich). The drugs were either present throughout the experiments or washed out at 120 min for Cyto B or Lat B after exosomes addition to show that the effects were reversible. Drug treatments did not result in a loss of cell viability. Inhibition of macropinocytosis or Clathrin-mediated internalization by EIPA or CPZ (Sigma-Aldrich), respectively, was performed as reported previously.

Electron microscopy

For ultrathin cell sections electron microscopy, exosomes were prelabeled with TfR antibody followed by conjugation of 12-nm protein A-gold, then either exosomes alone or together with phagocytic tracers was incubated with NIH 3T3 cells for 120 min or macrophages at 37°C for 10 min or 30 min, and washed by PBS. Cells were fixed with 2.5% glutaraldehyde for 30 min at room temperature followed by 1.5 h in 2% OsO4. Dehydration, embedding and thin sectioning (70 nm) were performed. Samples were stained and examined with transmission electron microscope (Philips).

Acknowledgments

We thank Dr. *Li Yu* (Tsinghua University, China) for constructive discussions on experimental design and manuscript preparations, *Jean Gruenberg* (University of Geneva, Switzerland) for antiserum against LBPA, *M. McNiven* (Mayo Clinic and Foundation, Rochester, USA), *Lucas Pelkmans* (ETH Zurich, Switzerland) for the dynamin constructs and *James Keen* (Thomas Jefferson University, Philadelphia, USA) for Clathrin-EGFP plasmids. Eps15 control and Eps15 EΔ 95/295 were kindly provided by Dr. *A. Benmerah* (INSERM, Paris, France) This work was supported by *National Natural Science Foundation of China (30830028) and National Basic Research Program of China (2010CB912400, 2010CD833706).*

Supporting Information

Additional Supporting Information may be found in the online version of this article:

Figure S1: Purification, characterization and labeling of exosomes. A) Exosomes purified on a sucrose cushion were negatively stained and observed by electron microscopy. Bar, 100 nm. B) Exosomes were further centrifuged on a continuous sucrose density gradient (0.25–2.5 M). Fractions collected from the top of the gradient were separated by SDS-PAGE and analyzed by western blotting for the exosomal markers Tsg101 and HSP70. The nonexosomal protein calnexin (ER) was detected in exosomal lysates. C) The sucrose density gradient-purified exosomes were labeled with PKH26 and visualized by confocal microscopy. Bar, 3 μm. D) Exosomes were immunolabeled with antibodies against Tsg101, TfR or control rabbit serum. Bound antibodies were detected with protein A-gold conjugates. Bars, 100 nm. E) MT4 cell-derived exosomes were

purified according to the procedures of K562 cell-derived exosomes and labeled with PKH67 fluorescent dye. Bar, 3 μm.

Figure S2: Exosomes do not colocalize with markers of the ER or Golgi. Cells were incubated with exosomes for 60 min, washed, stained by indirect immunofluorescence using a Golgi marker (Rab6) or an ER marker (calnexin), and analyzed by confocal microscopy. Bar, 5 μm

Figure S3: Exosomes do not enter caveolae or clathrin-coated vesicles during internalization. A) RAW 264.7 macrophages were incubated with exosomes for 10, 30 or 60 min. The samples were immuno-stained by anti-clathrin heavy-chain primary antibody and then labeled by FITC-conjugated second antibody. Coverslips were mounted by anti-fade solution (Roche) and visualized by laser scanning microscopy. Colocalization with clathrin was demonstrated by merging the fluorescent images. Scale bar, 8 μm. B) RAW 264.7 macrophages transfected with GFP-caveolin-1 were incubated with exosomes for 10 or 30 min. Representative confocal images are shown. Scale bar, 10 μm. C) Quantification of the colocalization with caveolae and clathrin-coated vesicles in macrophages at various time-points in at least 20 cells. The values given are the means ± SD of three independent experiments. Exo, exosome

Movie S1: Exosomes could be taken up by phagocytic cells. PKH26-labeled exosomes (red spots) from K562 cells were seen to move along the cell synapse first, and then into the macrophage (green) in the cell culture medium. Clathrin-GFP was moderately expressed in macrophage to show that the cell is alive. The video was recorded over about 10-min period at 37°C using real-time spinning disc confocal live-cell imaging microscopy (70 frames total). Magnification ×630.

Movie S2: Phagocytosed exosomes fuse with Rab7-containing compartments in microphages. Cells transfected with Rab7-GFP (green) were incubated with PKH26-exosomes (red) at 37°C for 15 min, washed and recorded for 60 min using a spinning disk confocal microscope system (300 frames total). Yellow spots indicate Rab7-positive vesicles that had already fused with exosomes.

Please note: Wiley-Blackwell are not responsible for the content or functionality of any supporting materials supplied by the authors. Any queries (other than missing material) should be directed to the corresponding author for the article.

References

1. Johnstone RM, Adam M, Hammond JR, Orr L, Turbide C. Vesicle formation during reticulocyte maturation. Association of plasma membrane activities with released vesicles (exosomes). J Biol Chem 1987;262:9412–9420.
2. Raposo G, Nijman HW, Stoorvogel W, Liejendekker R, Harding CV, Melief CJ, Geuze HJ. B lymphocytes secrete antigen-presenting vesicles. J Exp Med 1996;183:1161–1172.
3. Thery C, Regnault A, Garin J, Wolfers J, Zitvogel L, Ricciardi-Castagnoli P, Raposo G, Amigorena S. Molecular characterization of dendritic cell-derived exosomes. Selective accumulation of the heat shock protein hsc73. J Cell Biol 1999;147:599–610.
4. van Niel G, Raposo G, Candalh C, Boussac M, Hershberg R, Cerf-Bensussan N, Heyman M. Intestinal epithelial cells secrete exosome-like vesicles. Gastroenterology 2001;121:337–349.
5. Bard MP, Hegmans JP, Hemmes A, Luider TM, Willemsen R, Severijnen LA, van Meerbeeck JP, Burgers SA, Hoogsteden HC, Lambrecht BN. Proteomic analysis of exosomes isolated from human malignant pleural effusions. Am J Respir Cell Mol Biol 2004;31:114–121.
6. Fevrier B, Raposo G. Exosomes: endosomal-derived vesicles shipping extracellular messages. Curr Opin Cell Biol 2004;16:415–421.
7. Hegmans JP, Bard MP, Hemmes A, Luider TM, Kleijmeer MJ, Prins JB, Zitvogel L, Burgers SA, Hoogsteden HC, Lambrecht BN. Proteomic analysis of exosomes secreted by human mesothelioma cells. Am J Pathol 2004;164:1807–1815.
8. Simpson RJ, Lim JW, Moritz RL, Mathivanan S. Exosomes: proteomic insights and diagnostic potential. Expert Rev Proteomics 2009;6:267–283.
9. Johnstone RM. Exosomes biological significance: a concise review. Blood Cells Mol Dis 2006;36:315–321.
10. Pisitkun T, Shen RF, Knepper MA. Identification and proteomic profiling of exosomes in human urine. Proc Natl Acad Sci U S A 2004;101:13368–13373.
11. Pisitkun T, Johnstone R, Knepper MA. Discovery of urinary biomarkers. Mol Cell Proteomics 2006;5:1760–1771.
12. Caby MP, Lankar D, Vincendeau-Scherrer C, Raposo G, Bonnerot C. Exosomal-like vesicles are present in human blood plasma. Int Immunol 2005;17:879–887.
13. Keller S, Sanderson MP, Stoeck A, Altevogt P. Exosomes: from biogenesis and secretion to biological function. Immunol Lett 2006;107:102–108.
14. Vella LJ, Greenwood DL, Cappai R, Scheerlinck JP, Hill AF. Enrichment of prion protein in exosomes derived from ovine cerebral spinal fluid. Vet Immunol Immunopathol 2008;124:385–393.
15. Iero M, Valenti R, Huber V, Filipazzi P, Parmiani G, Fais S, Rivoltini L. Tumour-released exosomes and their implications in cancer immunity. Cell Death Differ 2008;15:80–88.
16. Pap E, Pallinger E, Pasztoi M, Falus A. Highlights of a new type of intercellular communication: microvesicle-based information transfer. Inflamm Res 2009;58:1–8.
17. Greco V, Hannus M, Eaton S. Argosomes: a potential vehicle for the spread of morphogens through epithelia. Cell 2001;106:633–645.
18. Abrami L, Liu S, Cosson P, Leppla SH, van der Goot FG. Anthrax toxin triggers endocytosis of its receptor via a lipid raft-mediated clathrin-dependent process. J Cell Biol 2003;160:321–328.
19. Zhang F, Sun S, Feng D, Zhao WL, Sui SF. A novel strategy for the invasive toxin: hijacking exosome-mediated intercellular trafficking. Traffic 2009;10:411–424.
20. Wiley RD, Gummuluru S. Immature dendritic cell-derived exosomes can mediate HIV-1 trans infection. Proc Natl Acad Sci U S A 2006;103:738–743.
21. Nguyen DG, Booth A, Gould SJ, Hildreth JE. Evidence that HIV budding in primary macrophages occurs through the exosome release pathway. J Biol Chem 2003;278:52347–52354.
22. Pelchen-Matthews A, Raposo G, Marsh M. Endosomes, exosomes and Trojan viruses. Trends Microbiol 2004;12:310–316.
23. Fevrier B, Vilette D, Laude H, Raposo G. Exosomes: a bubble ride for prions? Traffic 2005;6:10–17.
24. Fevrier B, Vilette D, Archer F, Loew D, Faigle W, Vidal M, Laude H, Raposo G. Cells release prions in association with exosomes. Proc Natl Acad Sci U S A 2004;101:9683–9688.
25. Valadi H, Ekstrom K, Bossios A, Sjostrand M, Lee JJ, Lotvall JO. Exosome-mediated transfer of mRNAs and microRNAs is a novel mechanism of genetic exchange between cells. Nat Cell Biol 2007;9:654–659.
26. Skog J, Wurdinger T, van Rijn S, Meijer DH, Gainche L, Sena-Esteves M, Curry WT Jr, Carter BS, Krichevsky AM, Breakefield XO. Glioblastoma microvesicles transport RNA and proteins that promote tumour growth and provide diagnostic biomarkers. Nat Cell Biol 2008;10:1470–1476.
27. Morelli AE, Larregina AT, Shufesky WJ, Sullivan ML, Stolz DB, Papworth GD, Zahorchak AF, Logar AJ, Wang Z, Watkins SC, Falo LD Jr, Thomson AW. Endocytosis, intracellular sorting, and processing of exosomes by dendritic cells. Blood 2004;104:3257–3266.
28. Lakkaraju A, Rodriguez-Boulan E. Itinerant exosomes: emerging roles in cell and tissue polarity. Trends Cell Biol 2008;18:199–209.
29. Stoorvogel W, Kleijmeer MJ, Geuze HJ, Raposo G. The biogenesis and functions of exosomes. Traffic 2002;3:321–330.
30. van Niel G, Porto-Carreiro I, Simoes S, Raposo G. Exosomes: a common pathway for a specialized function. J Biochem 2006;140:13–21.
31. Thery C, Zitvogel L, Amigorena S. Exosomes: composition, biogenesis and function. Nat Rev Immunol 2002;2:569–579.
32. Geminard C, Nault F, Johnstone RM, Vidal M. Characteristics of the interaction between Hsc70 and the transferrin receptor in exosomes released during reticulocyte maturation. J Biol Chem 2001;276:9910–9916.

33. Soderberg A, Barral AM, Soderstrom M, Sander B, Rosen A. Redox-signaling transmitted in trans to neighboring cells by melanoma-derived TNF-containing exosomes. Free Radic Biol Med 2007;43:90–99.
34. Kim SH, Bianco N, Menon R, Lechman ER, Shufesky WJ, Morelli AE, Robbins PD. Exosomes derived from genetically modified DC expressing FasL are anti-inflammatory and immunosuppressive. Mol Ther 2006;13:289–300.
35. Clement C, Tiwari V, Scanlan PM, Valyi-Nagy T, Yue BY, Shukla D. A novel role for phagocytosis-like uptake in herpes simplex virus entry. J Cell Biol 2006;174:1009–1021.
36. May RC, Machesky LM. Phagocytosis and the actin cytoskeleton. J Cell Sci 2001;114:1061–1077.
37. Spector I, Shochet NR, Blasberger D, Kashman Y. Latrunculins–novel marine macrolides that disrupt microfilament organization and affect cell growth: I. Comparison with cytochalasin D. Cell Motil Cytoskeleton 1989;13:127–144.
38. Schliwa M. Action of cytochalasin D on cytoskeletal networks. J Cell Biol 1982;92:79–91.
39. Gillooly DJ, Simonsen A, Stenmark H. Phosphoinositides and phagocytosis. J Cell Biol 2001;155:15–17.
40. Stephens L, Ellson C, Hawkins P. Roles of PI3Ks in leukocyte chemotaxis and phagocytosis. Curr Opin Cell Biol 2002;14: 203–213.
41. Miyanishi M, Tada K, Koike M, Uchiyama Y, Kitamura T, Nagata S. Identification of Tim4 as a phosphatidylserine receptor. Nature 2007;450:435–439.
42. Dasgupta SK, Abdel-Monem H, Niravath P, Le A, Bellera RV, Langlois K, Nagata S, Rumbaut RE, Thiagarajan P. Lactadherin and clearance of platelet-derived microvesicles. Blood 2009;113: 1332–1339.
43. Zakharova L, Svetlova M, Fomina AF. T cell exosomes induce cholesterol accumulation in human monocytes via phosphatidylserine receptor. J Cell Physiol 2007;212:174–181.
44. Scott CC, Botelho RJ, Grinstein S. Phagosome maturation: a few bugs in the system. J Membr Biol 2003;193:137–152.
45. Pitt A, Mayorga LS, Stahl PD, Schwartz AL. Alterations in the protein composition of maturing phagosomes. J Clin Invest 1992;90:1978–1983.
46. Gold ES, Underhill DM, Morrissette NS, Guo J, McNiven MA, Aderem A. Dynamin 2 is required for phagocytosis in macrophages. J Exp Med 1999;190:1849–1856.
47. de Camilli P, Takei K, McPherson PS. The function of dynamin in endocytosis. Curr Opin Neurobiol 1995;5:559–565.
48. Henley JR, Krueger EW, Oswald BJ, McNiven MA. Dynamin-mediated internalization of caveolae. J Cell Biol 1998;141:85–99.
49. Parton RG, Richards AA. Lipid rafts and caveolae as portals for endocytosis: new insights and common mechanisms. Traffic 2003;4:724–738.
50. Benmerah A, Bayrou M, Cerf-Bensussan N, Dautry-Varsat A. Inhibition of clathrin-coated pit assembly by an Eps15 mutant. J Cell Sci 1999;112:1303–1311.
51. Sun X, Yau VK, Briggs BJ, Whittaker GR. Role of clathrin-mediated endocytosis during vesicular stomatitis virus entry into host cells. Virology 2005;338:53–60.
52. West MA, Bretscher MS, Watts C. Distinct endocytotic pathways in epidermal growth factor-stimulated human carcinoma A431 cells. J Cell Biol 1989;109:2731–2739.
53. Kee SH, Cho EJ, Song JW, Park KS, Baek LJ, Song KJ. Effects of endocytosis inhibitory drugs on rubella virus entry into VeroE6 cells. Microbiol Immunol 2004;48:823–829.
54. Simons M, Raposo G. Exosomes–vesicular carriers for intercellular communication. Curr Opin Cell Biol 2009;21:575–581.
55. Ristorcelli E, Beraud E, Verrando P, Villard C, Lafitte D, Sbarra V, Lombardo D, Verine A. Human tumor nanoparticles induce apoptosis of pancreatic cancer cells. Faseb J 2008;22:3358–3369.
56. Tumne A, Prasad VS, Chen Y, Stolz DB, Saha K, Ratner DM, Ding M, Watkins SC, Gupta P. Noncytotoxic suppression of human immunodeficiency virus type 1 transcription by exosomes secreted from CD8+ T cells. J Virol 2009;83:4354–4364.
57. Khatua AK, Taylor HE, Hildreth JE, Popik W. Exosomes packaging APOBEC3G confer human immunodeficiency virus resistance to recipient cells. J Virol 2009;83:512–521.
58. Nolte-'t HE, Buschow SI, Anderton SM, Stoorvogel W, Wauben MH. Activated T cells recruit exosomes secreted by dendritic cells via LFA-1. Blood 2009;113:1977–1981.
59. Segura E, Nicco C, Lombard B, Veron P, Raposo G, Batteux F, Amigorena S, Thery C. ICAM-1 on exosomes from mature dendritic cells is critical for efficient naive T-cell priming. Blood 2005;106:216–223.
60. Clayton A, Turkes A, Dewitt S, Steadman R, Mason MD, Hallett MB. Adhesion and signaling by B cell-derived exosomes: the role of integrins. Faseb J 2004;18:977–979.
61. Mallegol J, van Niel G, Lebreton C, Lepelletier Y, Candalh C, Dugave C, Heath JK, Raposo G, Cerf-Bensussan N, Heyman M. T84-intestinal epithelial exosomes bear MHC class II/peptide complexes potentiating antigen presentation by dendritic cells. Gastroenterology 2007;132:1866–1876.
62. Parolini I, Federici C, Raggi C, Lugini L Palleschi S de Milito A Coscia C Iessi E Logozzi MA Molinari A Colone M Tatti M Sargiacomo M Fais S. Microenvironmental pH is a key factor for exosome traffic in tumor cells. J Biol Chem 2009; (In press).
63. Johnstone RM, Mathew A, Mason AB, Teng K. Exosome formation during maturation of mammalian and avian reticulocytes: evidence that exosome release is a major route for externalization of obsolete membrane proteins. J Cell Physiol 1991;147: 27–36.
64. Damm EM, Pelkmans L, Kartenbeck J, Mezzacasa A, Kurzchalia T, Helenius A. Clathrin- and caveolin-1-independent endocytosis: entry of simian virus 40 into cells devoid of caveolae. J Cell Biol 2005;168:477–488.
65. Gaidarov I, Keen JH. Phosphoinositide-AP-2 interactions required for targeting to plasma membrane clathrin-coated pits. J Cell Biol 1999;146:755–764.
66. Pelkmans L, Kartenbeck J, Helenius A. Caveolar endocytosis of simian virus 40 reveals a new two-step vesicular-transport pathway to the ER. Nat Cell Biol 2001;3:473–483.
67. Vitelli R, Santillo M, Lattero D, Chiariello M, Bifulco M, Bruni CB, Bucci C. Role of the small GTPase Rab7 in the late endocytic pathway. J Biol Chem 1997;272:4391–4397.